Research Article

Pulmonary Circulation

Right atrial mechanics provide useful insight in pediatric pulmonary hypertension

Kyle D. Hope, Renzo José Carlos Calderón Anyosa, Yan Wang, Andrea E. Montero, Tomoyuki Sato, Brian D. Hanna and Anirban Banerjee

Division of Cardiology, The Children's Hospital of Philadelphia, The Perelman School of Medicine at the University of Pennsylvania, Philadelphia, PA, USA

Abstract

Right atrial (RA) mechanics have been studied infrequently in children in the past due to technical constraints. With the advent of strain imaging, RA physiology can now be studied in greater detail. The principal aim of this study was to describe functional changes in right heart mechanics of children with idiopathic pulmonary arterial hypertension (PAH), by using new applications of RA strain. In this retrospective study, we evaluated RA mechanics of 20 patients (age range = 3–23 years) with PAH and 18 control patients. RA longitudinal strain (RALS) and longitudinal displacement (LD) were calculated by speckle-tracking echocardiography. RALS was plotted against LD, producing a characteristic strain-displacement (S-D) loop. Standard indices of right heart function and right heart catheterization data were obtained. Patients were clinically subdivided into "compensated" and "decompensated" PAH. A chart review was performed to identify patients who subsequently developed adverse outcomes, including death, awaiting or received lung and/or heart transplantation. RALS was significantly lower in decompensated PAH compared with both controls and compensated PAH. Area enclosed by S-D loops differed significantly between the compensated and decompensated PAH subgroups (5.33 [3.90–9.44] versus 1.83 [1.17–2.36], $P < 0.05$). S-D loop area and RALS possessed high sensitivity and specificity compared to other parameters for identifying children with PAH who subsequently developed adverse outcomes. In particular, their sensitivities and specificities were greatly superior compared to those of tricuspid annular plane systolic excursion (TAPSE). RALS may represent a useful metric for assessing right ventricular (RV) dysfunction. S-D loops, composed over an entire cardiac cycle, may present useful, composite information regarding both systolic and diastolic right heart function. RA mechanics may serve as useful tools for identifying patients with more severe PAH, who are at risk for future adverse outcomes associated with RV failure.

Keywords

pediatrics, pulmonary arterial hypertension, right atrial longitudinal strain, speckle tracking echocardiography, brain natriuretic peptide, six-minute walk, tricuspid annular systolic plane excursion, strain-displacement loop

Date received: 17 August 2017; accepted: 2 January 2018

Pulmonary Circulation 2018; 8(1) 1–10
DOI: 10.1177/2045893218754852

Introduction

Standard and advanced echocardiographic techniques continue to represent essential elements in the evaluation of patients with pulmonary hypertension (PAH). This disease process is characterized by increased pulmonary vascular resistance resulting in chronic right ventricular (RV) pressure overload, myocardial remodeling, leading to RV hypertrophy, dilation, and eventual RV failure.[1,2] The echocardiographic evaluation of a patient with suspected or established PAH may reveal characteristic findings such as tricuspid regurgitation (TR), right atrial (RA) and RV dilation, RV hypertrophy, abnormal shape and function of the interventricular septum, and dilation of the main pulmonary artery.[3] However, many of these findings may not be present

Corresponding author:
Anirban Banerjee, Division of Cardiology, The Children's Hospital of Philadelphia, 3401 Civic Center Boulevard, Philadelphia, PA 19104, USA.
Email: banerjeea@email.chop.edu

until quite late in the course of the disease, leading to the search for indices that may identify decompensation at earlier stages.

With the advent of speckle-tracking echocardiography (STE), it is now possible to quantify RA deformation over the course of the entire cardiac cycle from a single beat. Strain imaging has been applied in patients with PAH and right heart dysfunction.[4] In adults with chronic systolic heart failure, RA peak longitudinal strain (RALS) showed a strong inverse correlation with invasively measured systolic pulmonary artery pressure (PAP) and may represent an adjunct to invasive means of hemodynamic assessment.[5] In adults with PAH, RALS was noted to be low[6–8] and it negatively correlated with RA pressure.[7]

However, in the pediatric population the RA represents the ''forgotten'' chamber of the heart and studies on RA physiology and function in children are quite limited. This is especially true in pediatric PAH. STE can generate both strain and displacement data from the same heartbeat, which can simultaneously assess regional and global myocardial deformation of a cardiac chamber, including mechanical dyssynchrony. Simultaneous measurement of strain and displacement have been studied in other chambers of the heart, including the pressure-overloaded RV in adults. Notably, these studies in adults have shown that measurement of RV displacement and strain may facilitate reliable and quantitative estimation of RV function.[9,10] However, when the RV is significantly dilated, it may not be possible to include all the walls of the RV in the same echocardiographic acquisition window. The apex of the RV may often be truncated in acquisition windows, particularly in retrospective studies. In contrast, the RA is a simpler geometric structure and invariably well-visualized from an apical four-chamber view. Therefore, RA mechanics may provide a simpler and more reliable measure of RV decompensation. Based on these findings, we were enticed by the feasibility of describing a strain-displacement (S-D) relationship in the RA of children with PAH.

The objective of our study is to characterize RA function throughout a single cardiac cycle in healthy children and those with PAH, specifically looking at differences in RA strain and the strain-displacement relationship. We hypothesize that evaluation of RA strain in combination with RA displacement may provide useful insight into the function of both the normal and failing RA in PAH. These indices may identify patients at risk for future adverse outcomes.

Methods

Patient population

Patients followed at The Children's Hospital of Philadelphia with a diagnosis of PAH without post-tricuspid valve shunt were recruited for this study. Twenty children classified as having PAH due to idiopathic etiology (Nice Classification type 1.1), drug or toxin (Nice Classification type 1.3), congenital heart disease but without current shunt (Nice Classification type 1.4.4), or hematologic diagnosis (Nice Classification type 5.1)[3] were included in this study. We excluded PAH patients with significant defects in the atrial septum and patients with left ventricular (LV) dysfunction or pulmonary vein obstruction. Control individuals in this study were otherwise healthy pediatric patients referred for echocardiography for indications such as non-cardiac chest pain, vasodepressor syncope, and functional heart murmurs. All control participants were found to have structurally normal hearts without evidence of PAH by echocardiogram. This retrospective, descriptive study was approved by the Institutional Review Board of the Children's Hospital of Philadelphia.

Strain imaging

Echocardiograms were obtained using Philips iE33 ultrasound machines (Philips Medical Systems, Andover, MA, USA). Two-dimensional apical four-chamber views were obtained and uploaded for analysis by a vendor-independent STE software (Tomtec Cardiac Performance version 1.2.4.2, TomTec Imaging Systems, Munich, Germany). The frame rate of the acquired images exceeded 60 frames/s. Manual tracing along the RA endocardial border was performed with termination of the tracing 0.5 cm above the atrioventricular junction, to limit influence of tricuspid annular motion. The software divided the right atrium into six segments, with longitudinal strain and displacement obtained for each segment over a complete cardiac cycle. The global RA strain and longitudinal displacement (LD) for each patient were averages of the values obtained from these six segments. By convention, displacement away from the centroid of the cardiac chamber is indicated by negative values and may be considered as a surrogate for increase in RA volume.

Right-heart function

To better assess the utility of strain imaging in evaluation of right-sided function in individuals with PAH, the patients were subdivided into two groups: decompensated and compensated. ''Decompensated PAH'' was defined as the subgroup of patients with functional and laboratory evidence of significant right heart dysfunction at time of the echocardiogram. Specifically, the participants in this subgroup were in World Health Organization (WHO) functional class III or IV.[3] Based on adult and pediatric studies on brain natriuretic peptide (BNP), which showed strikingly decreased survival in idiopathic PAH, we chose a cut-off value for BNP of 180 pg/mL.[11,12] In our study, all decompensated PAH patients exhibited a BNP value of > 180 pg/mL. ''Compensated PAH'' was defined as individuals in WHO functional class I or II or a BNP < 180 pg/mL, or both.

In addition to RA mechanics and strain values, more conventional indices such as RV peak strain, RV area change (RVAC), and tricuspid annular plane systolic excursion (TAPSE) were recorded and used as indices of RV function. To compare TAPSE in participants of different ages and sizes, the values were indexed to the body surface area (BSA). We also compared percent-predicted TAPSE values using established reference ranges.[13–15] In individuals with PAH, BNP values obtained on or as close as possible to the date of the echocardiogram were evaluated for this study: BNP levels were obtained on 16 patients on the same day as the echocardiogram, the remaining four were obtained within three months.

Six-minute walk distances (6MWD) were obtained on or as close as possible to the date of the echocardiogram. Of the 20 PAH participants, 19 had 6MWD measurements recorded. Twelve measurements took place on the same day as the echocardiogram and four underwent the 6-min walking text (6MWT) within three months of their echocardiograms. For the remaining three individuals, the 6MWT was performed approximately six months after their echocardiograms. To determine a percent-predicted 6MWT value for each participant, the observed 6MWD was divided by the distance expected for their sex and age. Several reference ranges are available for pediatric 6MWT times based on their ages.[16–19] Using the appropriate reference ranges, we calculated predicted values for 6MWTs in our cohort.

Strain-displacement loops

Construction of S-D loops was undertaken by plotting RALS along the y-axis and LD along the x-axis. A typical S-D loop is illustrated in Fig. 2. The area enclosed by the S-D loop was calculated using the trapezoidal area of polygon formula, where the loop was broken into mini-trapezoids and the area of the loop was equal to the sum of all the trapezoids. The total area of the loop was the sum of $[x(i+1)–x(i)][y(i)+y(i+1))/2$ for i points of a polygon, where $x(1), y(1) = x(i+1), y(i+1)$.[20] The unit for this measurement is %.mm/cm and is simply referred to as unit (U) in this paper. In order to compare the right atria of children of different ages, the LD was indexed to the BSA. We used an additional method of indexing LD by dividing it with the largest RA dimension with the tricuspid valve closed.[21]

Cardiac catheterization data

We evaluated right heart catheterization data that were obtained within six months of the echocardiogram. Mean pulmonary artery pressure (mPAP) and indexed pulmonary vascular resistance (PVRi) were recorded for each individual.

Adverse outcomes

Based on > 2-year follow-up data, we identified participants who later developed adverse outcomes associated with their PAH. Adverse outcomes included death, awaiting or receiving lung and/or heart transplantation.

Statistical analysis

Continuous variables were non-normally distributed and are reported as median with interquartile ranges (IQR) noted parenthetically. Comparisons between the variables were performed using the Mann–Whitney U test. Non-parametric receiver operating characteristic (ROC) analysis was performed to test the sensitivity and specificity of the different echocardiographic indices, for the outcome described above. ROC curves were plotted and the areas under the curves were measured. For all significance testing, a difference was considered significant if P value < 0.05. The statistical analysis was performed using Stata software (StataCorp, version 13, College Station, TX, USA). Intra-class correlation (ICC) was used to assess intra- and inter-observer variability. For this purpose, eight patients were selected randomly and the analysis was repeated de novo by two investigators. For intra-observer variability, one observer repeated the measurements after two weeks.

Results

Demographics

A total of 38 children were included in this retrospective study, with 18 control individuals and 20 patients with PAH. Demographic data are summarized in Table 1. Control participants did not differ significantly from PAH participants with regards to age or BSA. Of the 20 PAH individuals, 15 were classified as idiopathic primary PAH (Nice Classification type 1.1), two were classified as having PAH arising due to connective tissue disease (Nice Classification type 1.4.1), one was classified as having PAH arising due to congenital heart disease (closed VSD) (Nice Classification type 1.4.4), one was classified as

Table 1. Demographic, clinical, and echocardiographic characteristics.

	Control	All PAH
n	18	20
Age (years)	12.83 ± 3.99	12.85 ± 6.02
Male	10 (55%)	9 (45%)
BSA (m^2)	1.48 ± 0.32	1.29 ± 0.43
WHO FC I		4
WHO FC II		6
WHO FC III		6
WHO FC IV		4

Data are expressed as mean ± standard deviation.
BSA, body surface area; FC, functional class; WHO, World Health Organization.

having PAH arising from drug or toxin (Nice Classification type 1.3), and one was classified as having PAH arising from hematologic etiology (Nice Classification type 5.1). None of the 20 individuals with PAH included in this study were found to have a post-tricuspid valve shunt. A small patent foramen ovale with bidirectional shunting was noted in two patients.

Comparison of control and PAH population

The control group differed significantly from the PAH group in several RV parameters, including percent-predicted TAPSE, and RV to LV ratio in diastole. RV longitudinal strain was lower in the PAH group versus controls ($-15.7 \pm 3.6\%$ vs $-23.3 \pm 3.8\%$, $P < 0.05$; data expressed as mean ± standard deviation). Several indices of RA function were abnormal in the PAH group. Notably, RALS was significantly decreased in the PAH group compared to controls (31.9 [21.6–48.1] versus 57.8 [52.9–65.9], $P < 0.05$.). RALS also showed a moderately significant inverse correlation with mPAP in patients undergoing catheterization within six months ($r = 0.51$, $P < 0.05$) (Fig. 1). The above findings are summarized in Table 2.

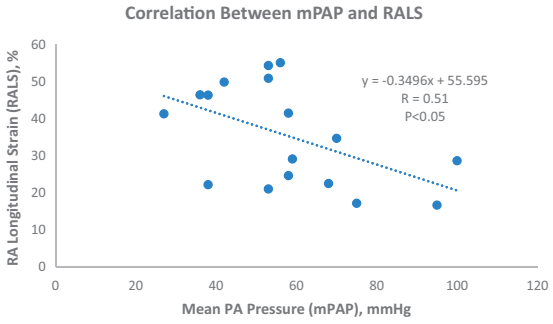

Fig. 1. Mean PAP shows an inverse correlation with RA peak longitudinal strain.

The S-D loop had a characteristic elliptical shape and counterclockwise rotation, and was reflective of the reservoir, conduit, and contractile phases of RA function (Fig. 2). The reservoir phase began with tricuspid valve closure (TVC) and continued until the tricuspid valve opened (TVO). The conduit phase began at TVO and was followed by a brief contractile (booster pump) phase. The contractile phase in children is not as pronounced as in adults and manifested only a subtle incisura on the strain curves. Therefore, the contractile (booster pump) phase was not calculated separately in our study. When indexed for RA lengths, the areas enclosed by S-D loops were significantly decreased in the group consisting of all PAH patients compared to control participants (3.8 [1.9–8.5] versus 7.9 [5.9–9.9], $P < 0.05$).

Comparison of compensated and decompensated PAH groups

The entire PAH population was divided into compensated and decompensated groups to determine if RA indices such as RALS and S-D loops varied between these subgroups and whether a point of decline in RA function could be detected in these individuals. The data are summarized in

Table 2. Right heart data.

	Control	All PAH	Compensated PAH	Decompensated PAH
N	18	20	13	7
RALS (%)	57.84 (52.94–65.89)	31.93 (21.61–48.19)*	46.38 (34.71–50.94)*	21.04 (17.17–22.53)*†
Loop area^{BSA} (U)	25.31 (15.07–29.53)	12.95 (10.44–32.19)	19.30 (13.68–38.21)	10.22 (5.41–11.60)*†
Loop area^{length} (U)	7.88 (5.94–9.88)	3.85 (1.92–8.51)*	5.33 (3.90–9.44)	1.83 (1.17–2.36)*†
TAPSE^{BSA} (cm)	1.45 (1.30–1.83)	1.26 (1.16–1.69)	1.23 (1.17–1.56)	1.49 (0.75–1.69)
%p TAPSE (%)	91.24 (84.97–102.69)	81.71 (68.59–85.76)*	83.79 (76.97–85.88)*	73.02 (61.85–83.67)*
LV:RV^{diastole}	1.88 (1.66–2.05)	1.52 (0.98–1.94)*	1.73 (1.1–2.19)	0.84 (0.61–1.52)*†
BNP (pg/mL)		60.5 (19.95–300.85)	29.7 (15.8–52.7)	434.5 (190.5–509.5)†
6MWD (m)		548 (412–595)	574.5 (486–617.5)	440 (336–560)
%p 6MWD (%)		89.2 (75.09–96.59)	94.17 (90.69–101.71)	75.09 (66.89–81.81)†
mPAP (mmHg)		56 (42–68)	54.5 (40–58.5)	68 (53–75)
PVRi (Wood Units. m^2)		9.2 (9.1–21.6)	13.9 (8.4–18.5)	18.1 (14.1–25.5)

Data are expressed as median with first and third interquartile range in parenthesis.
*P value < 0.05 when compared with control.
†P value < 0.05 when compared with compensated PAH.
RALS, right atrial longitudinal strain; Loop area^{BSA}, S-D loop area indexed for body surface area; Loop area^{length}, S-D loop area indexed for right atrial length; TAPSE^{BSA}, tricuspid annular plane systolic excursion, indexed for body surface area; %p TAPSE, percent-predicted TAPSE; RV:LV^{diastole}, ratio of right ventricular to left ventricular diameter at end-diastole; BNP, brain natriuretic peptide; 6MWD, 6-min walk distance; %p 6MWD, percent-predicted 6-min walk distance; mPAP, mean pulmonary artery pressure.

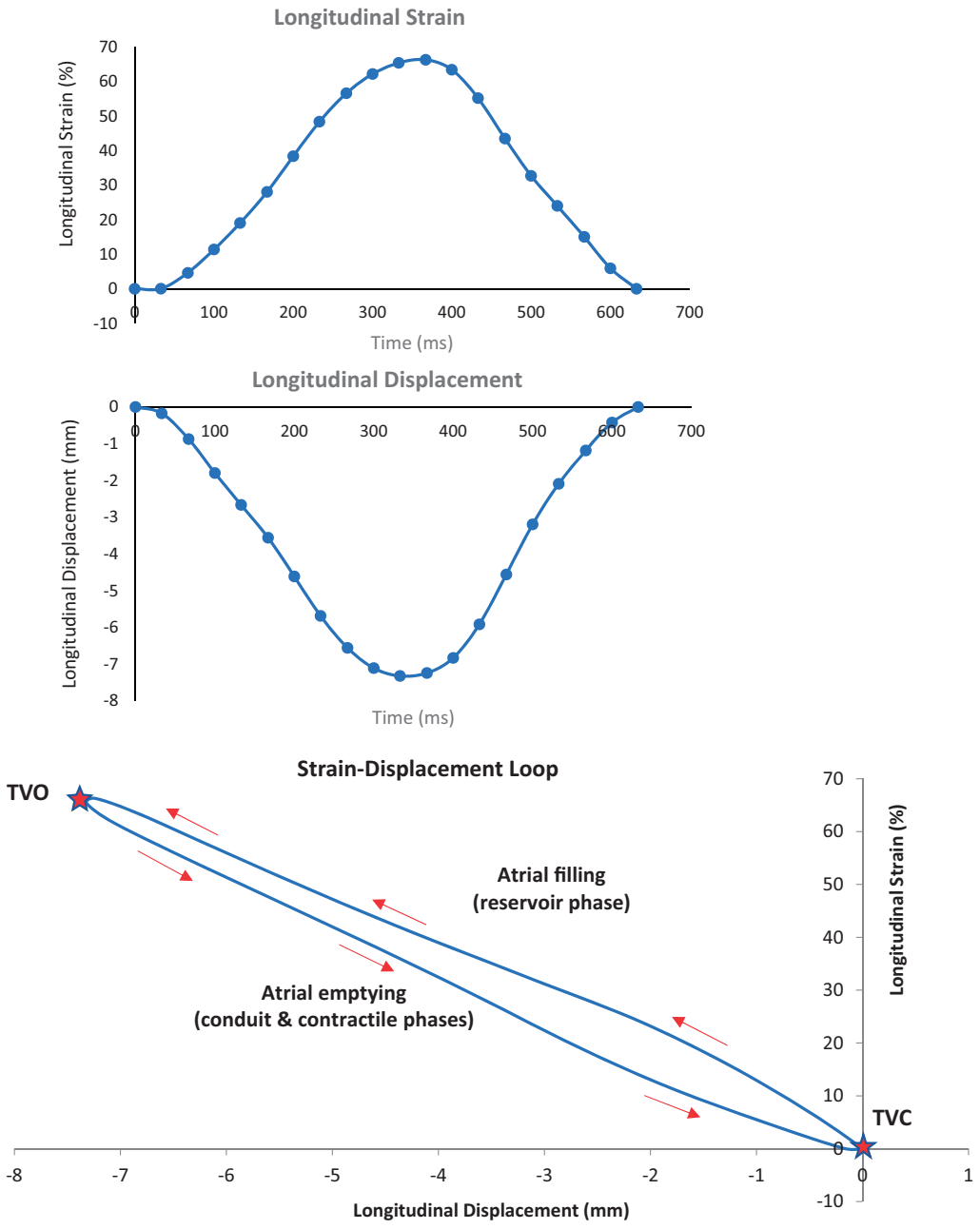

Fig. 2. Typical RA S-D loop. The S-D loop is generated by plotting the RA LD along the x-axis and the longitudinal strain along the y-axis. This results in a characteristic elliptical loop in the counter-clockwise direction, starting with tricuspid valve closure (TVC). The area of the S-D loop was constituted by reservoir, conduit, and contractile phases of RA function. The reservoir phase continues from TVC to tricuspid valve opening (TVO), after which starts the conduit phase, followed by a brief contractile phase. The contractile phase in children is not as pronounced as in adults and therefore a distinct incisura is not well-detected in the waveforms of pediatric patients.

Table 2. Regarding the more conventional data, it is noteworthy that the BNP values exceeded 190 pg/mL in all patients in the decompensated group (median = 434.5 pg/mL). The decompensated PAH participants differed significantly from the compensated PAH group with regards to several measures of RA mechanics (RALS, S-D loop area indexed for either BSA or RA length), RV mechanics (RV to LV ratio in diastole), laboratory markers, and clinical function (percent-predicted 6MWT) as outlined in Table 2. Both the compensated and decompensated PAH populations exhibited elevated mPAPs. Despite a trend of observing higher mPAP and PVRi in the decompensated group, there was no statistical difference in mPAP or PVRi between the two subgroups.

We wish to point out that the area enclosed by the S-D loop was similar between the control and compensated

groups, but significantly smaller in the decompensated PAH patients compared with both control and compensated PAH individuals (Fig. 3, Table 2).

Outcomes in PAH populations

Six out of seven decompensated and one out of 13 compensated participants experienced an adverse outcome. To determine the sensitivity and specificity in identifying the individuals who later went on to develop these outcomes, ROC curves were constructed for RALS, S-D loop area indexed for BSA, S-D loop area indexed for RA length, BNP, percent-predicted TAPSE, and TAPSE indexed for BSA (Table 3). ROC curves for S-D loop indexed for RA length and BSA, and RALS all demonstrated excellent AUC (0.92, 0.90, 0.92, respectively), whereas the AUC for TAPSE indexed for BSA was quite poor (0.54) (Fig. 4).

Intra-observer and inter-observer variability

We found excellent reproducibility for RALS and LD measurements. ICC values for inter-observer variability were 0.88

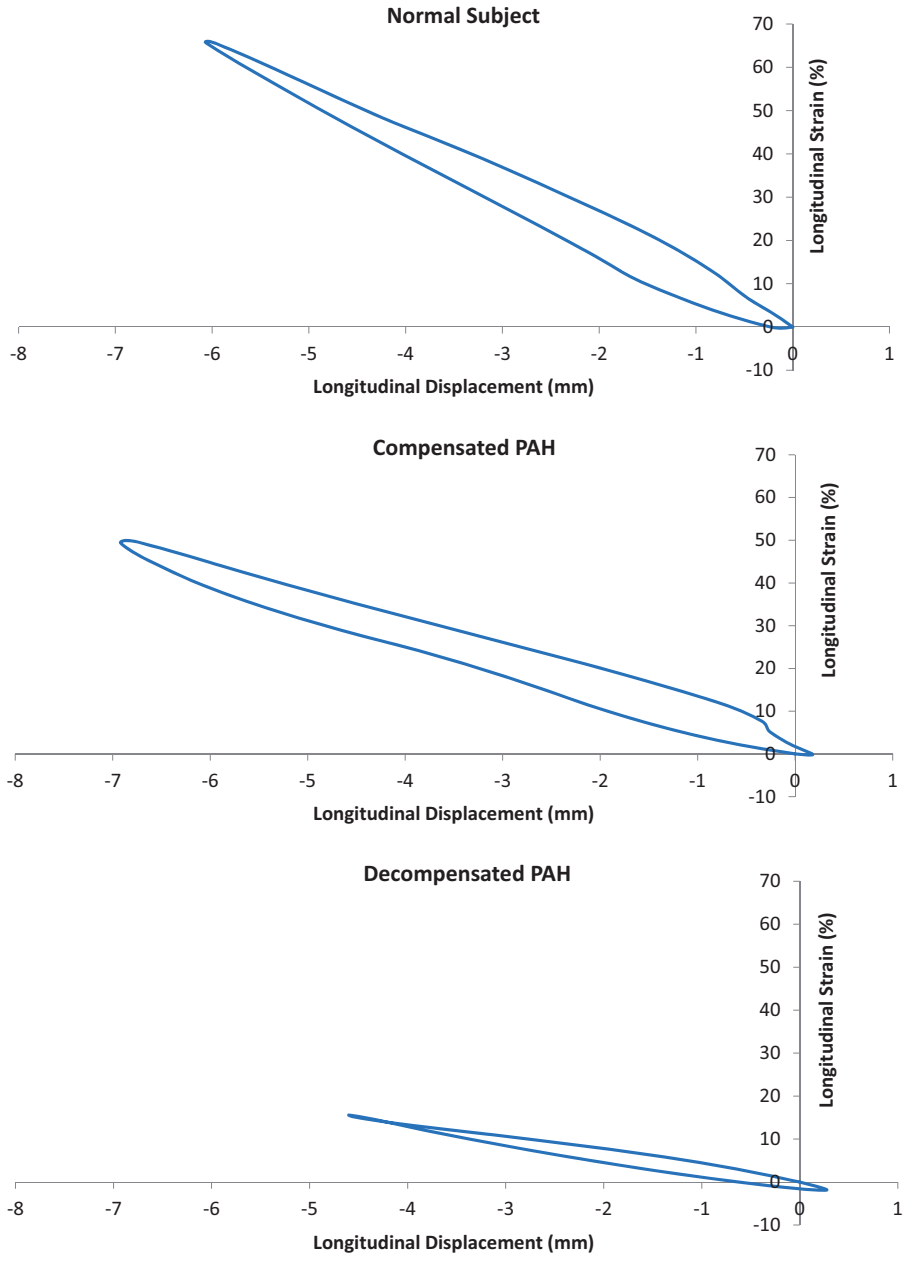

Fig. 3. Characteristic appearance of S-D loops in a normal subject, compensated PAH, and decompensated PAH. The area enclosed by the S-D loop is notably smaller in decompensated PAH, but not in compensated PAH. Here LD is indexed for body surface area. Gradually increasing negative values of LD indicate filling of RA.

Table 3. ROC curve data for measures of right heart function and adverse outcomes.

ROC analysis	Cutpoint	Sensitivity (%)	Specificity (%)	AUC	95% CI
Loop area^{length} vs. Outcome	2.36 U	100	92.3	0.92	0.77–1.0
Loop area^{BSA} vs. Outcome	11.6 U	100	84.6	0.90	0.75–1.0
RALS vs. Outcome	28.74%	100	84.6	0.92	0.79–1.0
BNP vs. Outcome	190.4 pg/mL	85.7	92.3	0.84	0.58–1.0
Percent-predicted TAPSE vs. outcome	83.7%	85.71	53.85	0.64	0.35–0.92
TAPSE indexed for BSA vs. outcome	1.27 cm	71.4	61.5	0.54	0.23–0.84

AUC, area under ROC curve; Loop area^{length}, S-D loop area indexed for right atrial length; Loop area^{BSA}, S-D loop area indexed for body surface area; RALS, right atrial longitudinal strain; BNP, brain natriuretic peptide; CI, confidence interval.

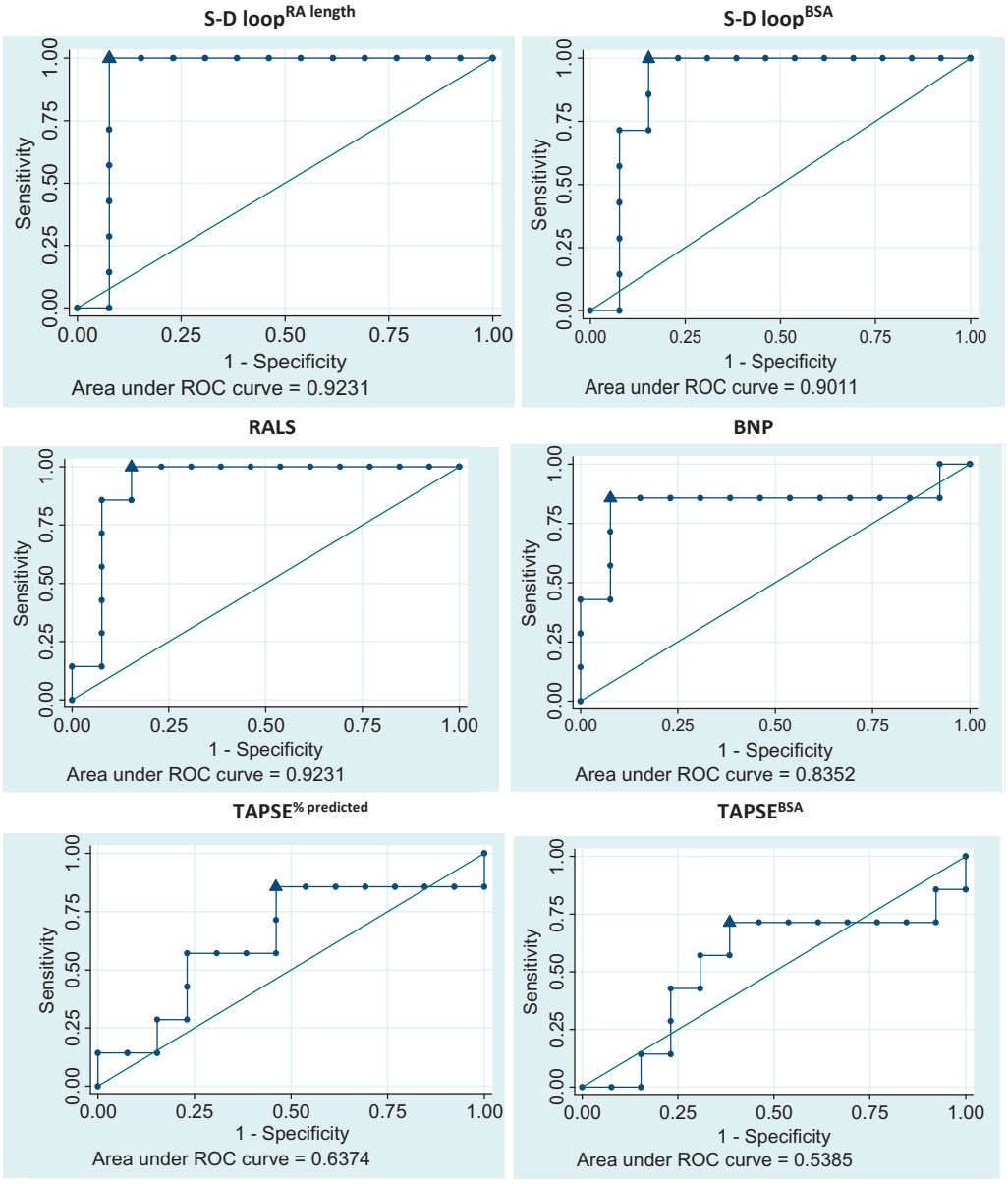

Fig. 4. ROC curves comparing (a) S-D loop area indexed for RA length vs outcome, (b) S-D loop area indexed for BSA vs outcome, (c) RALS vs outcome, (d) BNP vs outcome, (e) percent-predicted TAPSE vs outcome, and (f) TAPSE indexed for BSA vs outcome. Additional data for each ROC curve (cut-point, sensitivity, specificity, area under curve [AUC]) can be found in Table 3. In all ROC curves, cut-points are delineated by triangles.

for RALS and 0.94 for LD, whereas ICC values for intra-observer variability were 0.9 for RALS and 0.92 for LD, respectively.

Discussion

Although the RA is often regarded as the ''forgotten chamber'' of the heart, RA mechanics may serve as an important barometer of right heart dysfunction. Strain imaging represents an exciting new tool for evaluating RA mechanics. This single-center, pilot study represents one of the first efforts to use this tool in the evaluation of pediatric PAH. Additionally, in this study we have proposed a new concept, the S-D loop, that may provide useful discriminatory information regarding compensated and decompensated states of PAH in children.

Right atrial longitudinal strain

Measurement of RA strain may represent an exciting new tool in the assessment of RA physiology that was not available in the past. Previous research into pediatric RA strain have demonstrated abnormal indices in single ventricle patients[22] and in patients with repaired tetralogy of Fallot.[23] Adult studies have demonstrated a decreased RALS in participants with PAH compared with controls[6,7] and this finding is reflected in our pediatric data. Of interest, RALS was also significantly different between compensated and decompensated subgroups of PAH.

Patients with chronic right heart pressure overload demonstrate diastolic dysfunction before systolic dysfunction.[24] The gradual increase in RA strain is reflected by the ascending limb and peak of the RA strain curve (Fig. 2). This phase occurs during atrial filling, referred to as reservoir function of the RA. Atrial filling, in turn, occurs during ventricular diastole. Therefore, the lower RALS in patients with PAH may reflect the abnormal myocardial relaxation and diastolic dysfunction of the RV.

Atrial strain-displacement loops

To gain insights into RA function and mechanics over the entire cardiac cycle, we propose a novel approach, the S-D loop. Plotting atrial longitudinal strain against LD produced a characteristic elliptical loop, with turning points corresponding to tricuspid valve closing and opening (Fig. 2). Strain represents local deformation of a small myocardial segment, whereas displacement evaluates the movement of the whole chamber. Moreover, displacement may serve as a surrogate for change in RA volume. The S-D loops may serve as a helpful index, comparing atrial segmental deformation against the overall movement of the atrial wall and may provide a useful ''composite view'' of atrial filling (reservoir phase) and emptying (conduit + contractile phases). The concept of simultaneous measurement of longitudinal strain and LD has been applied in adults with constrictive pericarditis,[25] RV pressure overload,[9,10] LV pressure overload in aortic stenosis,[26] and in the evaluation of carotid artery stiffness.[27] Longitudinal strain and LD have been used to describe the elasticity of the dilated aorta. Elasticity of the aorta incorporates both the property of dilating and the property of recoiling to its initial shape.[28] Similarly, the atrial S-D relationship may provide indirect evidence of the elasticity of the RA tissue. We also speculate that during the conduit phase (when tricuspid valve remains open), the RA S-D loop may also reflect RV diastolic stiffness. The concept of the S-D loop is quite new. It provides simultaneous information regarding the regional shortening and global movement of the atrial wall during the entire cardiac cycle. The concept was derived from torsion-displacement loop described by us and others.[28,29] To describe the area enclosed by torsion-volume loops, Notomi et al. coined the term ''Filling Work.'' They proposed that the area enclosed by the loops gives a measure of ''work'' being performed by the chamber and may provide a measure of the energy stored in the cardiac chamber.[30] Although a theoretical analogy is being drawn, we cannot extrapolate these theoretical concepts to our study, as ours is a pilot study that aimed to show the feasibility of constructing strain versus displacement loops in normal and diseased RA. Clearly, further work is needed to determine the physiologic significance of the area enclosed by the S-D loop. Based on other studies that have used strain and displacement simultaneously, we can merely speculate that the reduced area of the S-D loop may provide a visual display of the decreased elasticity of the atrial tissue. It is a first step in visually describing the RA mechanics during an entire cardiac cycle. This was nicely demonstrated in patients with decompensated PAH, where the S-D loops were notably ''skinnier'' (Fig. 3, lower panel).

Comparison with current means of assessing right heart mechanics in PAH

Non-invasive identification of impending RV decompensation is challenging in children with PAH, since the 6MWD and the degree of TR do not deteriorate with increase in disease severity at the same rate as in adult PAH. Moreover, in the absence of sufficient TR, current echocardiographic indices are poor predictors of disease severity. In this scenario, RA mechanics may provide a better insight into the state of RV decompensation. Both RALS and S-D loops may serve as upgrades to the clinician's toolkit. It is important to recognize the best use of each tool available for the evaluation of PAH in children. It may be that a combination of tools will yield the most complete picture of right heart mechanics at a given point in time. This study and others in adults[6,7] have demonstrated that the decrease in RALS with increasing disease severity makes RALS a useful measure of RV diastolic dysfunction. Since diastolic dysfunction of the RV precedes systolic dysfunction in chronic right heart pressure overload,[22] RALS may be a useful index

to monitor serial diastolic changes in patients with PAH, similar to findings in serum BNP. In contrast, TAPSE and RV strain provide serial evaluation of RV during systole, while the RA S-D loop may provide a composite insight into both systolic and diastolic function of RV. Our study showed that the RA indices had greater sensitivity and specificity (and larger AUCs) compared to the more conventional indices like BNP and TAPSE. In our study, out of all the indices evaluated, the S-D loop indexed for RA length showed the best sensitivity (100%) and specificity (92.3%). This points to great potential value of this index but also warrants further validation. In particular, serial monitoring of these indices after initiating therapy for PAH would be of utmost interest to researchers and clinicians alike.

Clinical implications

Established clinical criteria used in the evaluation of adult PAH may be less useful in the pediatric population. For example, the 6MWT can be difficult to carry out according to established protocols in younger children and does not always reflect the degree of right heart dysfunction. Children often present with lower RA pressures, better compensation of the RV to the increased afterload, and higher mixed venous oxygen saturations.[2,13] The study of RA mechanics may therefore be of value in this population. The S-D loop provides us with a composite view of the reservoir, conduit, and contractile phases of RA function. The mathematical calculations for measuring these new indices can be incorporated into calculation packages of commercial echocardiography machines. Automation of RALS and S-D loops into commercial ultrasound machines may encourage more use of these indices in busy clinical settings and not limit them to the research arena only.

Study limitations

Due to small sample size, further subgroup analyses were not feasible. Furthermore, statistical evaluations determining degree of association between the laboratory variables and adverse outcomes were not performed because of small sample size. We excluded individuals with ongoing lung parenchymal lesions, significant atrial level shunts, pulmonary vein stenoses, and LV dysfunction. In this fashion, we present a relatively homogeneous population which should have narrow limits for test results and clinical outcomes. Moreover, even in a tertiary referral center, idiopathic PAH remains an uncommon disease. As our primary aim in this study was to perform research on a new echocardiographic index, we pursued a statistically sufficient number of patients needed to provide meaningful results, at the same time limiting heterogeneity in the sample. This study is a single-center, pilot study that may pave the way for larger, multicenter studies. The primary focus of this study was on the RA physiology. Therefore, we did not focus significantly on the RV physiology.

Conclusions

RA mechanics may serve as novel metrics in the assessment of right heart dysfunction in children with PAH. Identification of impending RV decompensation is difficult in pediatrics, where sub-maximal exercise testing and the degree of TR are often better than expected for the degree of elevated mPAP. RA strain and S-D loops may serve as useful tools for identifying patients at risk for future adverse outcomes from progressive RV dysfunction.

Conflict of interest

The author(s) declare that there is no conflict of interest.

Funding

This research was funded by the Madeline Schwamm Memorial Fund for Pediatric Pulmonary Hypertension Research.

References

1. Vonk-Noordegraaf A, Haddad F, Chin KM, et al. Right heart adaptation to pulmonary arterial hypertension: physiology and pathobiology. *J Am Coll Cardiol* 2013; 62: D22–33.
2. Barst RJ, Ertel SI, Beghetti M, et al. Pulmonary arterial hypertension: a comparison between children and adults. *Eur Respir J* 2011; 37: 665–677.
3. Galiè N, Humbert M, Vachiery JL, et al. 2015 ESC/ERS Guidelines for the diagnosis and treatment of pulmonary hypertension: The Joint Task Force for the Diagnosis and Treatment of Pulmonary Hypertension of the European Society of Cardiology (ESC) and the European Respiratory Society (ERS): Endorsed by: Association for European Paediatric and Congenital Cardiology (AEPC), International Society for Heart and Lung Transplantation (ISHLT). *Eur Heart J* 2016; 37(1): 67–119.
4. Kannan A, Poongkunran C, Jayaraj M, et al. Role of strain imaging in right heart disease: a comprehensive review. *J Clin Med Res* 2014; 6: 309–313.
5. Padeletti M, Cameli M, Lisi M, et al. Right atrial speckle tracking analysis as a novel noninvasive method for pulmonary hemodynamics assessment in patients with chronic systolic heart failure. *Echocardiography* 2011; 28: 658–664.
6. Querejeta Roca G, Campbell P, Claggett B, et al. Right atrial function in pulmonary arterial hypertension. *Circ Cardiovasc Imaging* 2015; 8(11): e003521.
7. Sakata K, Uesugi Y, Isaka A, et al. Evaluation of right atrial function using right atrial speckle tracking analysis in patients with pulmonary artery hypertension. *J Echocardiogr* 2016; 14: 30–38.
8. Fukuda Y, Tanaka H, Ryo-Koriyama K, et al. Comprehensive functional assessment of right-sided heart using speckle tracking strain for patients with pulmonary hypertension. *Echocardiography* 2016; 33: 1001–1008.
9. Urheim S, Cauduro S, Frantz R, et al. Relation of tissue displacement and strain to invasively determined right ventricular stroke volume. *Am J Cardiol* 2005; 96: 1173–1178.
10. Ichikawa K, Dohi K, Sugiura E, et al. Ventricular function and dyssynchrony quantified by speckle-tracking echocardiography in patients with acute and chronic right ventricular pressure overload. *J Am Soc Echocardiogr* 2013; 26: 483–492.

11. Nagaya N, Nishikimi T, Uematsu M, et al. Plasma brain natriuretic peptide as a prognostic indicator in patients with primary pulmonary hypertension. *Circulation* 2000; 102: 865–870.
12. Bernus A, Wagner BD, Accurso F, et al. Brain natriuretic peptide levels in managing pediatric patients with pulmonary arterial hypertension. *Chest* 2009; 135(3): 745–751.
13. Jone PN and Ivy DD. Echocardiography in pediatric pulmonary hypertension. *Front Pediatr* 2014; 2: 124.
14. Koestenberger M, Ravekes W, Everett AD, et al. Right ventricular function in infants, children and adolescents: reference values of the tricuspid annular plane systolic excursion (TAPSE) in 640 healthy patients and calculation of z score values. *J Am Soc Echocardiogr* 2009; 22: 715–719.
15. Rudski LG, Lai WW, Afilalo J, et al. Guidelines for the echocardiographic assessment of the right heart in adults: a report from the American Society of Echocardiography endorsed by the European Association of Echocardiography, a registered branch of the European Society of Cardiology, and the Canadian Society of Echocardiography. *J Am Soc Echocardiogr* 2010; 23: 685–713.
16. Lammers AE, Hislop AA, Flynn Y, et al. The 6-minute walk test: normal values for children of 4-11 years of age. *Arch Dis Child* 2008; 93: 464–468.
17. Li AM, Yin J, Au JT, et al. Standard reference for the six-minute-walk test in healthy children aged 7 to 16 years. *Am J Respir Crit Care Med* 2007; 176: 174–180.
18. Iwama AM, Andrade GN, Shima P, et al. The six-minute walk test and body weight-walk distance product in healthy Brazilian subjects. *Brazilian J Med Biol Res* 2009; 42: 1080–1085.
19. Chetta A, Zanini A, Pisi G, et al. Reference values for the 6-min walk test in healthy subjects 20–50 years old. *Respir Med* 2017; 100: 1573–1578.
20. Area of a trapezoid. 2012. Available at: http://www.aaamath.com/geo78_x5.htm (last accessed 9 April 2017).
21. Nawaytou HM, Yubbu P, Montero AE, et al. Left ventricular rotational mechanics in children after heart transplantation. *Circ Cardiovasc Imaging* 2016; 9: e004848.
22. Khoo MS, Smallhorn JF, Kaneko S, et al. The assessment of atrial function in single ventricle hearts from birth to Fontan: a speckle-tracking study by using strain and strain rate. *J Am Soc Echocardiogr* 2013; 26: 756–764.
23. Kutty S, Shang Q, Joseph N, et al. Abnormal right atrial performance in repaired tetralogy of Fallot: A CMR feature tracking analysis. *Int J Cardiol* 2017; 248: 136–142.
24. Gaynor SL, Maniar HS, Bloch JB, et al. Right atrial and ventricular adaptation to chronic right ventricular pressure overload. *Circulation* 2005; 112: I212–218.
25. Negishi K, Popović ZB, Negishi T, et al. Pericardiectomy is associated with improvement in longitudinal displacement of left ventricular free wall due to increased counterclockwise septal-to-lateral rotational displacement. *J Am Soc Echocardiogr* 2015; 28: 1204–1213.
26. Cramariuc D, Gerdts E, Davidsen ES, et al. Myocardial deformation in aortic valve stenosis: relation to left ventricular geometry. *Heart* 2010; 96(2): 106–112.
27. Tat J, Au JS, Keir PJ, et al. Reduced common carotid artery longitudinal wall motion and intramural shear strain in individuals with elevated cardiovascular disease risk using speckle tracking. *Clin Physiol Funct Imaging* 2017; 37: 106–116.
28. Bieseviciene M, Vaskelyte JJ, Mizariene V, et al. Two-dimensional speckle-tracking echocardiography for evaluation of dilative ascending aorta biomechanics. *BMC Cardiovasc Disord* 2017; 17(1): 27.
29. Di Maria MV, Caracciolo G, Prashker S, et al. Left ventricular rotational mechanics before and after exercise in children. *J Am Soc Echocardiogr* 2014; 27(12): 1336–1343.
30. Notomi Y, Martin-Miklovic MG, Oryszak SJ, et al. Enhanced ventricular untwisting during exercise: a mechanistic manifestation of elastic recoil described by Doppler tissue imaging. *Circulation* 2006; 113(21): 2524–2533.